SDSS'Rio 2010 STABILITY AND DUCTILITY OF STEEL STRUCTURES
E. Batista, P. Vellasco, L. de Lima (Eds.)
Rio de Janeiro, Brazil, September 8 - 10, 2010

IMPERFECTIONS SENSITIVITY ANALYSIS OF PITCHED ROOF COLD – FORMED STEEL PORTAL FRAMES

Dan Dubina*, Viorel Ungureanu*, Zsolt Nagy, Luis Nunes* and Paul Pernes****

* Faculty of Civil Engineering, The "Politehnica" University of Timisoara, Romania
e-mails: dan.dubina@ct.upt.ro, viorel.ungureanu@ct.upt.ro

** Faculty of Civil Engineering, The Technical University of Cluj-Napoca, Romania
e-mail: zsolt.nagy@gordias.ro

Keywords: Imperfections, Pitch roof portal frames, Thin-walled cold-formed steel members, Bolted joints, Numerical simulations, Full-scale test, General Method for lateral and lateral-torsional buckling.

Abstract. *The paper summarizes the results of experimental and numerical simulation programs carried out on full-scale pitched roof cold-formed steel portal frames of back-to-back lipped channel sections with bolted joints in order to evaluate the influence of different type of geometrical and structural imperfections on the structural stability performance of these structures. Double frame units have been tested under: (1) horizontal load, and (2) horizontal and gravity loadings. For numerical simulations the imperfections were taken according to the tolerances specified in EN 1090-2 and the provisions of EN 1993-1-1. Based on this, in case of partially lateral restrained frames, the accuracy of General Method of EN1993-1-1 is investigated.*

1 INTRODUCTION

The global behavior of cold-formed steel portal frames of bolted joints were studied experimentally by Lim [1], Dundu & Kemp [2] and Kwon et al. [3]. All these studies provided evidence of the crucial importance of joint performance on the global response of frames, which are semi-rigid and in almost all cases with partial strength [1].

An extensive experimental program on ridge and eaves joints, with three alternative joint configurations, using welded bracket elements and bolts installed either on webs only or both on webs and flanges was carried out at the "Politehnica" University of Timisoara. Test on joints have shown their failure occurs always at the edge of lap between connecting bracket and cold-formed sections. In case of specimens with bolts on webs only, the failure starts early by local bucking of the web, caused by the high concentration of compression stresses around bolt holes, and subsequently is extended on the flanges, to form at the end a local plastic mechanism. Specimens of bolts installed both on the flanges and webs of connected members are nearly full resistant, but still remain semi-rigid. Detailed results on joint behavior are reported by Dubina et al. [4]. Based on experimental results, a calculation procedure based on the component method [5] was adapted for cold-formed joints [6]. Joint stiffness and moment capacity, obtained using the component method, are used to develop a joint model for global structural analysis. Two full-scale tests on cold-formed pitched-roof portal frames with bolted joints were performed, with the primary objective to assess their performance under horizontal (seismic) loading. A procedure to evaluate the ultimate design capacity of these frames was proposed [7]. In present paper, results of experimental investigations together with numerical simulations and comparison with analytical predictions are presented. For numerical simulations the imperfections were taken according to the tolerances specified in EN 1090-2 and the provisions of EN 1993-1-1. Based on this, in case of partially lateral restrained frames, the accuracy of General Method of EN1993-1-1 is investigated.

2 FRAME TESTING AND PREVIOUS NUMERICAL ANALYSIS

Following experimental tests on cold-formed joints, two full-scale tests on frames were performed [8]. Frames dimensions were chosen identical to the ones in the initial design used to establish the dimensions of tested joints. Considering the poor performance of joints with bolts on web only, configurations with both web and flange bolts were used for frame construction. Pinned supports were designed at the column bases. Objective of the full-scale tests was to assess performance of pitched-roof cold-formed portal frames with moment-resisting joints under horizontal loading, with particular emphasis on earthquake loading. The test setup consisted of two frames in upward position, located 1.5m apart. Tie bracings were provided between the two frames in order to provide out-of plane stability. Purlins and corrugated sheeting were installed on the girders, but no side rails were provided on the columns. Therefore, the structural systems can be considered as laterally restraint. The schematic representation of test setup is shown in Figure 1. A reaction frame was used in order to apply lateral load.

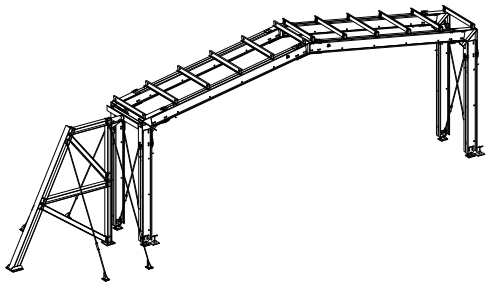

Figure 1: Experimental test setup for full-scale tests.

In the case of the first test (C1) only lateral loading was applied. For the second test (C2), gravity loading corresponding to seismic design situation was applied, followed by increasing lateral load up to failure. Total gravity loading amounted to 31.2kN per frame, and was applied using 30 corrugated steel sheets laid on the purlins.

Experimental tests on ridge and eaves joints showed that bolted connections of back-to-back lipped channel cold-formed members are semi-rigid, even when bolts are provided on the web and flanges of the lipped channel section. Therefore, deformations can be underestimated if connections are assumed rigid for global frame analysis. In order to assess the influence of connection stiffness and post-buckling resistance, three frame models, presented in Figure 2, were analyzed [8]. A nonlinear static analysis under increasing lateral load, performed with SAP2000 computer code, was applied to the models and the results were compared to experimental ones.

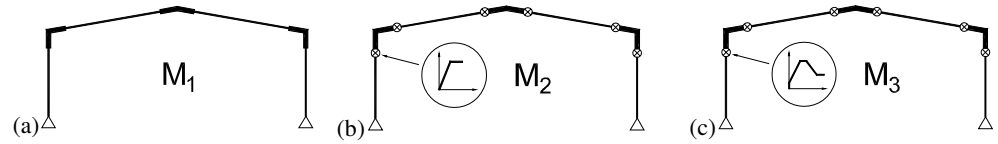

Figure 2: Considered structural models: (a) rigid connections – M1, (b) elastic-perfectly plastic connections – M2 and (c) degrading connections – M3.

The first model (M1, see Figure 2a) was the model where connections were considered rigid. Nominal geometrical characteristics were used to model members. Finite dimensions of brackets were taken into account. Local buckling of members was modeled by rigid-plastic hinges located at the extremities of cold-formed members. Analytically determined moment capacity (M_c=117.8kNm) was considered. The second model (M2, see Figure 2b) was obtained from model M1 by adopting an elastic

perfectly-plastic model of the joint. Initial stiffness (K_{iniC}=5224kNm/rad) and moment capacity (M_c=117.8kNm) were the ones obtained using the analytical procedure. In the case of M3 model (see Figure 2c), the elasto-plastic model of the joint was enhanced considering the stiffening effect due to the wedging and friction between the cold-formed profiles and the bracket in the early stage of loading. Also, the softening branch in the post-elastic stage was considered. Value of the "slipping" moment M_s was estimated based on experimental results, as 15% from the connection moment capacity. Following the initial rigid behavior, connection model consists of an elastic response at the initial stiffness K_{iniC} (determined using component method), up to the connection moment capacity M_C.

Figures 3 and 4 show and display the behavior and response of C1 frame. It can be observed that the rigid model (M1) provides a good approximation of the initial response of the frame up to lateral forces of about 10kN. At larger forces, model M2, with semi-rigid connections, provides a better approximation of the experimental response. The M3 model, incorporating both the initial rigid response and subsequent semi-rigid behavior shows the best agreement to the experimental results.

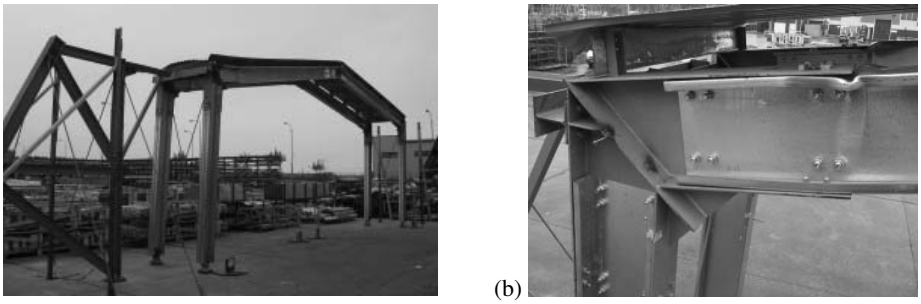

(a) (b)

Figure 3: C1 frame: (a) global view and (b) local buckling of the left beam connection.

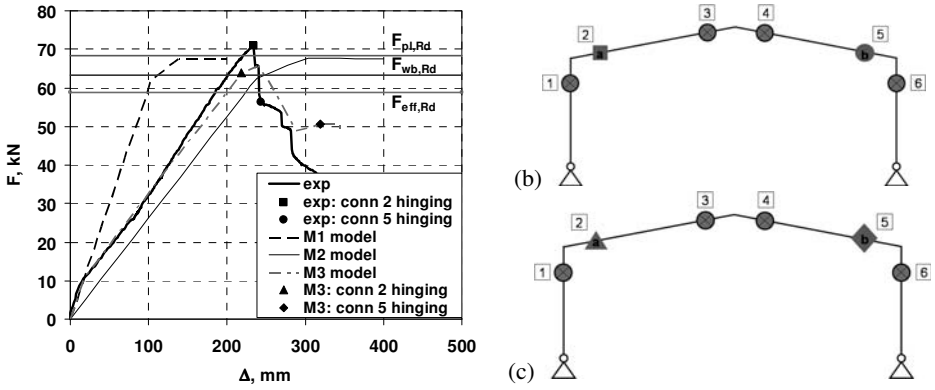

Figure 4: Frame C1: (a) experimental vs. numerical lateral force – deformation curves, (b) position of local buckling observed experimentally and (c) in the numerical model.

In the case of the C2 frame, gravity loading corresponding to seismic design situation was first applied, followed by increasing lateral loading up to complete failure of the frame. Figures 5 and 6 show similar behavior and results as in case of C1 frame. However, global resistance under horizontal loading was smaller in the case of the C2 frame. It was attained at the first local buckling in the beam near the right eaves (connection 5, Figure 6b), when the lateral force resistance dropped suddenly. It was followed by a combined local buckling and lateral-torsional buckling of one of the columns at the mid-height (see Figure 5a). Finally, local buckling of the beam at the left eaves was observed (at connection 2, Figure 6b).

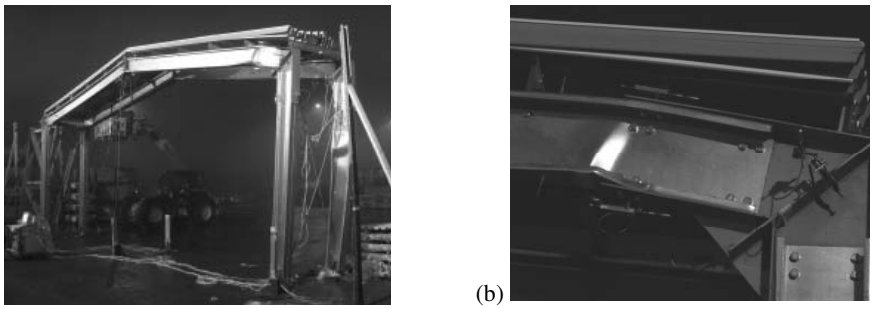

Figure 5: C2 frame: (a) global view and (b) local buckling of the right beam connection.

All numerical models overestimate global frame resistance under lateral loading. The location of first local buckling was correctly predicted by numerical model (at connection 5, see Figure 6c), column hinging observed in the experimental test was not confirmed by numerical models. Column hinging can be explained by the fact that in the experimental test the horizontal load had an eccentricity of 25mm, which increased the influence of compression force in right side column, combined with the effect of no lateral restraining at column flanges by side rails. These effects were not present in the numerical model.

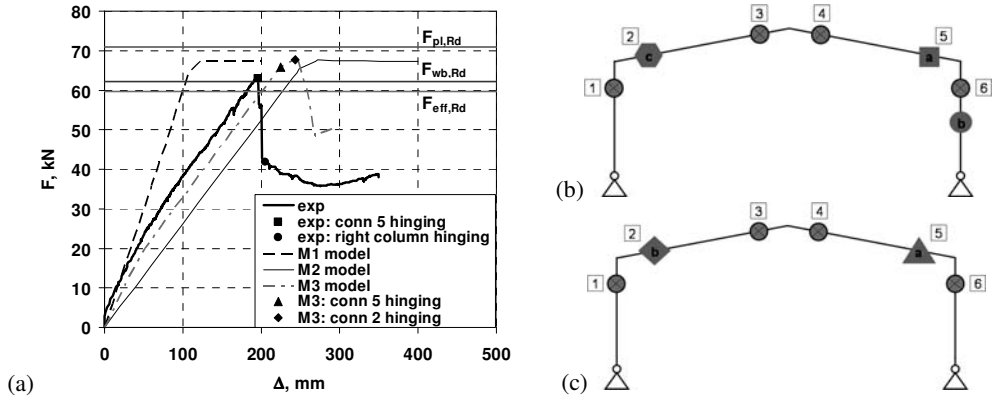

Figure 6: Frame C2: (a) comparison of experimental and numerical lateral force - deformation curves, (b) position of local buckling observed experimentally and (c) in the numerical model.

It can be concluded that the M3 model seems to provide the best agreement to the experimental results, if initial stiffness, lateral resistance, and post-buckling response are envisaged. Global frame resistance under lateral loads drops quickly after the first local buckling, when maximum force is reached.

As analytical prediction of design capacity, three methods were proposed to estimate the ultimate resistance [7] at the edge of bracket-to-rafter lap (e.g. the first local buckling location) of that section under design loads, i.e.:

- the "effective width" model, $F_{eff,Rd}$, based on EN1993-1-3 procedure;
- the "plastic" model, based on the local plastic mechanism, $F_{pl,Rd}$;
- the "interactive" model, which considers the coupling effect between web crippling, at the edge of the bracket-to-member lap, and the bearing in the bolt holes in flanges, $F_{wb,Rd}$.

In Figures 4(a) and 6(a) the three lines, corresponding to the three methods are presented comparatively with tests and numerical simulations. As expected, the "interactive" model, fit better with tests and numerical analysis (M3 model).

3 GENERAL METHOD FOR LATERAL AND LATERAL TORSIONAL BUCKLING OF STRUCTURAL COMPONENTS

The General Method of EN1993-1-1 [10] may be used where the other methods of EN1993-1-1 do not apply. It allows the verification of the resistance to lateral and lateral-torsional buckling for structural components. Overall resistance to out-of-plane buckling for any structural component can be verified by:

$$\frac{\chi_{op}\alpha_{ult,k}}{\gamma_{M1}} \geq 1.0 \tag{1}$$

where: $\alpha_{ult.k}$ is the minimum load amplifier of the design loads to reach the characteristic resistance of the most critical cross-section of the structural component considering its in plane behavior without taking lateral or lateral-torsional buckling into account however accounting for all effects due to in plane geometrical deformation and imperfections, global and local, where relevant; χ_{op} is the reduction factor for the non-dimensional slenderness $\bar{\lambda}_{op}$, to take account of lateral and lateral-torsional buckling; γ_{M1} is the safety coefficient ($\gamma_{M1} = 1$).

The global non dimensional slenderness $\bar{\lambda}_{op}$ for the structural component should be determined from:

$$\bar{\lambda}_{op} = \sqrt{\frac{\alpha_{ult,k}}{\alpha_{cr,op}}} \tag{2}$$

where: $\alpha_{cr.op}$ is the minimum amplifier for the in plane design loads to reach the elastic critical resistance of the structural component with regards to lateral or lateral-torsional buckling without accounting for in plane flexural buckling. In determine $\alpha_{cr.op}$ and $\alpha_{ult.k}$, Finite Element analysis may be used.

4 NUMERICAL ANALYSIS

4.1 Numerical analysis

A GMNIA FE model was calibrated based on experimental tests. One frame only from the set of two was considered in the analysis (i.e. a plane frame with partial lateral restraints). FE models have been prepared for each experimental test, e.g.: (1) one for the first experimental test (C1), where only lateral loading (seismic effect) was applied at left eaves up to failure and, (2) another one for the second experimental test (C2), where constant gravity loading was applied, simulating the dead and snow loads corresponding to seismic load combination, followed by the lateral load up to failure. ABAQUS/CAE v.6.8 was used for these numerical simulations. The features of the FE model used in the study are: (1) *4-node shell element (S4R)* used to model the cold-formed members; (2) *3D solid elements (C3D4)* to model the brackets at the eaves and ridge; (3) *nonlinear spring elements* to model the effect of purlins (two springs are used to model the lateral restrains introduced by purlins of type Z150/1); (4) *contact elements* to model the gap between the back-to-back cold-formed lipped channels. The mesh size for the shell elements was around 24x24mm. For the analyses the connections were assumed to be rigid. The material properties for thin-walled cold-formed elements, determined from coupon tests, are: yield strength of 486N/mm^2, ultimate tensile strength 553N/mm^2, Young's modulus E=210000N/mm^2 and a measured thickness minus zinc coating of 2.93mm. Based on tests results, the material has been introduced by means of bilinear isotropic elastic-perfectly plastic model.

Few imperfections were measured on site, and only for C2 tested frames; they are synthetically presented in Figure 7. There are no measured imperfections for frame C1 and no measured imperfections at the level of members for both tested frames. However, for numerical analyses, global and local imperfections have been considered according with: (1) tolerances proposed by EN1090-2 [11] or (2) equivalent imperfections for structural analyses proposed by EN1993-1-1 [10]. The following types of imperfections have been taken into account: a) global imperfections for frames; b) local imperfections for individual members (in- & out-of-plane imperfections); c) imperfections at the level of cross-section.

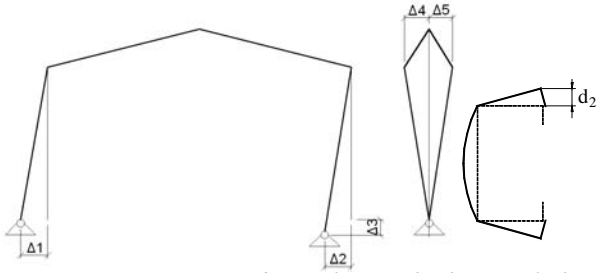

Frame C2.1	Frame C2.2
Δ_1 = 16mm	Δ_1 = 0mm
Δ_2 = 20mm	Δ_2 = 1mm
Δ_3 = 6mm	Δ_3 = 11mm
Δ_4 = 4.76mm	Δ_4 = 3.82mm
Δ_5 = 3.59mm	Δ_5 = 4.67mm

d_2 = 1.9mm

Figure 7: Measured imperfections for frames C2 (for arrangement see Figure 1).

Based on preliminary analyses, in order to emphasize the importance of imperfections shape, only the imperfections presented in Figure 8 were considered. These are summarized in Table 1 too. It should be observed that the measured imperfections are covered by the imperfections proposed by the codes.

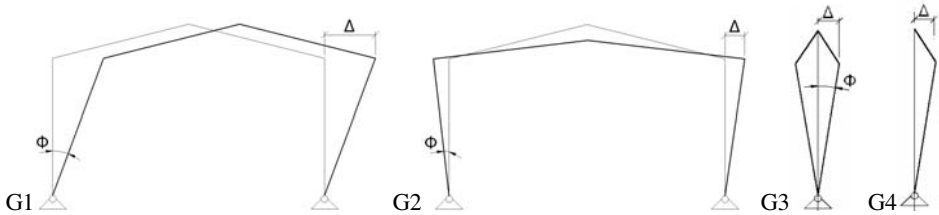

a) global imperfections for frames (G)

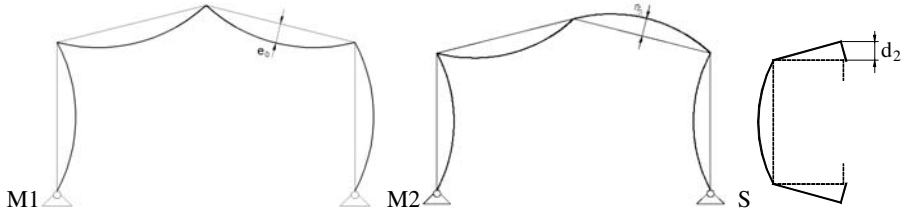

b) local imperfections (M) for individual members (in- & out-of-plane); c) section imperfection (S)

Figure 8: Types of imperfections for GMNIA FE model.

Table 1: Values of imperfections according to EN1090-2 and EN1993-1-1.

	Frame	*Columns in-plane*	*Columns out-of-plane*	*Cross-section*
EN1090-2	$\Delta = h/500$	$\pm h/750$	$\pm h/750$	$d_2 = t$
[mm]	*8.2*	*5.5*	*5.5*	*3*
EN1993-1-1	$\phi = \phi_o \cdot \alpha_h \cdot \alpha_m$	$\pm h/250$	$\pm h/200$	$d_2 = t$
[mm]	*20.5*	*16.8*	*21*	*3*

Table 2 shows the sensitivity of frame C1, subjected only to a horizontal load applied to left eaves, to different types of imperfections (single or coupled) according with the shapes presented in Figure 8. The sizes of imperfections for this parametric study were taken according with EN1090-2, and are given in Table 1. It should be observed that the analyzed frame is not sensible to imperfections, the difference being less than 3%.

Table 2: Sensitivity to imperfections of frame C1.

Type of imperfection	*No imperf.*	*G1*	*G2*	*G3*	*G4*	*M1*	*M2*	*S*	*G1M1S in plane*
F_{max} *(kN)*	*73.932*	*73.364*	*73.366*	*72.859*	*72.169*	*73.179*	*73.192*	*72.611*	*72.634*

On the following, a more complex combination of imperfections was considered in order to compare the numerical model with the experimental one, both for frame C1 and frame C2. This combination of imperfections was considered according to the types of imperfections measured on site for frame C2; it is the *G1M1S* model which combines the in- and out-of-plane imperfections, taken according with EN1090-2 and EN1993-1-1 (see Table 1). Figure 9 displays the experimental and numerical curves. A good agreement at the level of ultimate force for frame C1 can be observed. For frame C2, the difference in ultimate force can be explained by the fact that in the experimental test the horizontal load has been applied with an eccentricity of 25mm, which increased the influence of compression force in right side column, and due to the fact that there were no lateral restraining at column flanges by side rails, it induced at the end a localized instability form (see Figure 5a). This imperfection was not considered in the numerical model. The difference in slope of the experimental and numerical curves is due to the fact that in the present models the eaves and ridge connections were considered fully rigid. The values of ultimate horizontal loads are summarized in Table 3.

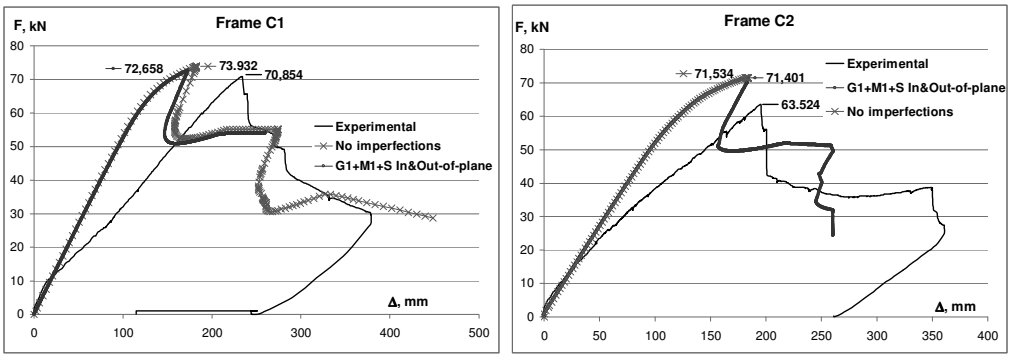

Figure 9: Experimental vs. numerical G1M1S curve.

Table 3: Frames C1 and C2: comparison of experimental and numerical ultimate forces.

	Experimental F_u *(kN)*	*EN1090-2 imperfections* $F_{EN1090\text{-}2}$ *(kN)*	*EN1090-2 imperfections* $F_{EN1993\text{-}1\text{-}1}$ *(kN)*
Frame C1	*70.85*	*72.658*	*72.629*
Frame C2	*63.52*	*71.401*	*71.316*

Figure 10 shows the deformed shape of nonlinear elastic-plastic (*G1M1S*) model and local plastic mechanism formed at the edge of bracket-to-rafter lap for Frame C1, similar with the experimental one presented in Figure 5b.

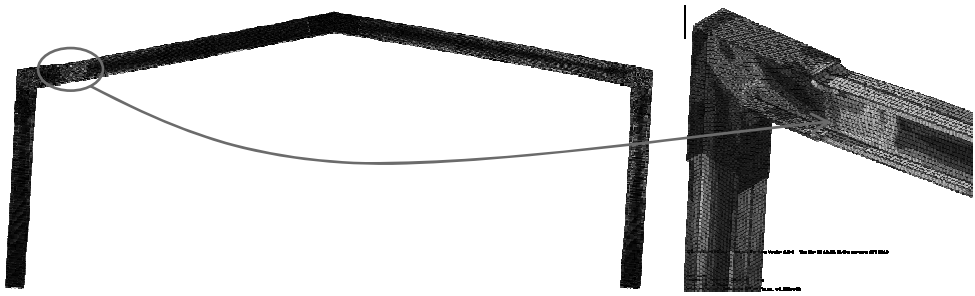

Figure 10: Frame C1: nonlinear elastic-plastic model and local plastic mechanism.

4.2 LEA and in-plane GMNIA for General Method of EN1993-1-1

Both linear eigen buckling (LEA) and in-plane nonlinear elastic-plastic (GMNIA) analyses have been applied for C1 and C2 frames, in order to validate the General Method. The imperfections taken according to EN1090-2 for in-plane GMNIA analyses are those given in Table 1. Table 4 presents the results obtained via General Method, for the safety coefficient $\gamma_{M1} = 1$, and shows that, at least for the case of these frames (stiff enough), it gives good results.

Table 4: Frames C1 and C2: General Method.

	GMNIA in-plane $\alpha_{ult,k}$	*LEA* $\alpha_{cr,op}$	$\overline{\lambda}_{op}$	χ_{op}	$\chi_{op}\alpha_{ult,k} / \gamma_{M1} \geq 1$
Frame C1	*1.224*	*3.990*	*0.554*	*0.859*	*1.051*
Frame C2	*1.191*	*4.148*	*0.536*	*0.868*	*1.033*

5 CONCLUSION

Frames tested experimentally under horizontal loading only, and horizontal and gravity loadings have been studied using GMNIA FE model. For numerical simulations the imperfections were taken according with the tolerances specified EN1090-2 and the provisions of EN1993-1-1. Different types of imperfections were considered. For the analyzed frames, designed for current load conditions in Romania (heavy snow, moderate earthquake), the results prove they are less sensitive to imperfections. In the next step, the General Method of EN1993-1-1 was applied to the analyzed frames and the obtained results encourage to recommend to use this approach for such a type of structures because it is simply enough and effective.

REFERENCES

[1] Lim, J.B.P., *Joint effects in cold-formed steel portal frames*. Nottingham Univ., PhD Thesis, 2001.

[2] Dundu, M. and Kemp, A.R., "Strength requirements of single cold formed channels connected back-to-back". *Journal of Constructional Steel Research*, **62**(3), 250-261, 2006.

[3] Kwon, Y.B., Chung, H.S. and Kim, G.D., "Experiments of cold-formed steel connections and portal frames". *Journal of Structural Engineering*, **132**(4), 600-607, 2006.

[4] Dubina, D., Stratan, A., Ciutina, A., Fulop, L. and Nagy, Zs., "Performance of ridge and eaves joints in cold-formed steel portal frames", *Proc. of the 17th International Specialty Conference*, Orlando, Florida, USA, 727-742, 2004.

[5] EN1993-1-8. *Eurocode 3: Design of Steel Structures – Part 1-8. Design of joints*. European Committee for Standardization, Brussels, 2005.

[6] Nagy, Zs., Stratan, A. and Dubina, D., "Application of component method for bolted cold-formed steel joints". *Proc. of International Conference on Metal Structures – ICMS 2006 "Steel – A new and traditional material for building"*, Poiana Brasov, Romania, 207-215, 2006.

[7] Dubina, D., Ungureanu, V. and Stratan A., "Ultimate design capacity of pitch-roof portal frames made by thin-walled cold-formed members", *Proc. of the 5th Int. Conf. on Thin-Walled Structures: Recent Innovations and Developments*, Gold Coast, Australia, Vol. 1, 387-394, 2008.

[8] Dubina, D., Stratan, A. and Nagy, Zs., "Full – scale testing of cold-formed steel pitched-roof portal frames of back-to-back channel sections and bolted joints". *Proc. of the Sixth International Conference on Steel and Aluminum Structures*, Oxford, UK, 931-939, 2007.

[9] EN1993-1-3. *Eurocode 3 – Part 1-3: Supplementary rules for cold-formed thin gauge members and sheeting*. European Committee for Standardization, Brussels, 2006.

[10] EN1993-1-1. *Eurocode 3: Design of steel structures – Part 1-1: General rules and rules for buildings*. European Committee for Standardization, Brussels, 2005.

[11] EN1090-2. *Execution of steel structures and aluminium structures. Technical requirements for the execution of steel structures*. European Committee for Standardization, Brussels, 2008.